MEASUREMENTS AND ANALYSIS OF CAVITY MICROPHONICS AND FREQUENCY CONTROL IN THE CORNELL ERL MAIN LINAC PROTOTYPE CRYOMODULE*

M. Ge†, N. Banerjee, J. Dobbins, R. Eichhorn, F. Furuta, G. Hoffstaetter, M. Liepe, P. Quigley, J. Sears, V. Veshcherevich, Cornell University, Ithaca, New York, USA.

Abstract

The Cornell Main Linac cryomodule (MLC) is a key component in the CBETA project. The SRF cavities with high loaded-Q in the MLC are very sensitive to microphonics from mechanical vibrations. Poor frequency stability of the cavities would dramatically increase the input RF power required to maintain stable accelerating fields in the SRF cavities. In this paper, we present detailed results from microphonics measurement for the cavities in the MLC, discuss dominant vibration sources, and show vibration damping results. The current microphonics level meets the CBETA requirement of a 36MeV energy gain without applying fast tuner compensation.

INTRODUCTION

The Cornell-BNL FFAG-ERL Test Accelerator (CBETA) [1, 2] is designed and now under construction at Cornell University to prove the FFAG-ERL concept for BNL's future Nuclear Physics facility, eRHIC [3]. One of the important components in CBETA is the Cornell Main Linac Cryomodule (MLC) prototype [4-6] which will provide 36MeV energy gain for a single-turn beam of the CBETA. The MLC consists of six 1.3GHz 7-cell SRF cavities. However there are several effects that can limit the cavity accelerating voltages in beam operation below their ultimate quench limit. Microphonics, known as frequency perturbation of SRF cavities, is one of the main sources of field perturbation, driving the RF power required for high Q_{ext} cavity operation in an ERL. If we only consider the effect of microphonics, the relation between the required RF forward power ($P_{forward}$) and the frequency detuning ($\Delta\omega = \omega_c - \omega$) at an accelerating voltage (V_{acc}) is determined by Eq. (1) [7],

$$P_{forward} = \frac{V_{acc}^2}{4 \cdot R/Q \cdot Q_L} \cdot \frac{\beta+1}{\beta}\left\{1+\left(2Q_L \cdot \frac{\Delta\omega}{\omega}\right)^2\right\}, \quad (1)$$

where R/Q is the ratio of cavity shunt impedance (R) to its intrinsic quality factor (Q_0), Q_L is the loaded quality factor, β is the coupling coefficient which is defined by Eq. (2),

$$\beta \equiv \frac{Q_0}{Q_{ext}} = \frac{Q_0}{Q_L} - 1, \quad (2)$$

and Q_{ext} is the external quality factor of the input power coupler. The Q_{ext} for the MLC is $\sim 6 \times 10^7$. Comparing to $Q_0 \sim 2 \times 10^{10}$, gives a β of about 1000. Thus $Q_L \approx Q_{ext} \sim 6 \times 10^7$.

It can be seen from Eq. (1) that the RF power is approximately proportional to the square of frequency detuning ($\Delta\omega$), i.e. $P_{forward} \sim (\Delta\omega)^2$, for large detuning. Hence poor frequency stability demands significantly more RF power to sustain the cavity at an accelerating voltage. The maximum output of the High Power RF Amplifiers (HPA) driving the cavities of the MLC is 5kW per cavity; nominally, the RF amplifiers should work at 2 to 3 kW to leave sufficient overhead for residual beam loading compensation.

MICROPHONICS MEASUREMENTS

Experimental Set-up

The location of the MLC and 2K pumping skid in the testing area (L0E) is shown in Fig. 1. The pumping skid is about 15m away from the MLC. The position of the six cavities in the MLC is shown in Fig. 1 (insert). The cavities #1, #3, and #5 are un-stiffened cavities; and the cavities #2, #4, and #6 have mechanical stiffening rings between the cells [8]. The chimney from the 2K two-phase (2K2P) line to the helium-gas return pipe is located between cavities #3 and #4.

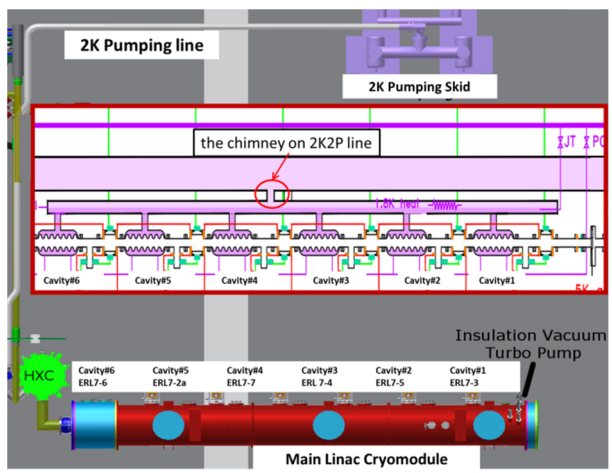

Figure 1: Cryogenic operation diagram of the MLC with the 2K pumping skid and 2K pumping line. The position of the cavities in the MLC is shown in the middle subplot.

The microphonics measurements were carried out when the cavities were cooled to temperature of 1.8K with the resonant frequency tuned to 1300MHz, but without applying any fast tuner compensation; the accelerating gradients (E_{acc}) of the cavities was set to ~1.3MV/m.

* Work supported by NSF Grant NSF DMR-0807731
† mg574@cornell.edu

The block diagram of the low level RF (LLRF) system for a 7-cell cavity is illustrated in Fig. 2 a). Microphonics will cause large phase perturbations, thus the LLRF system adopts a digital in phase and quadrature (IQ) field feedback controller instead of a traditional amplitude and phase controller. The photograph of the system is shown in Fig. 2 b). More technical details of the LLRF system can be found in Ref. [7].

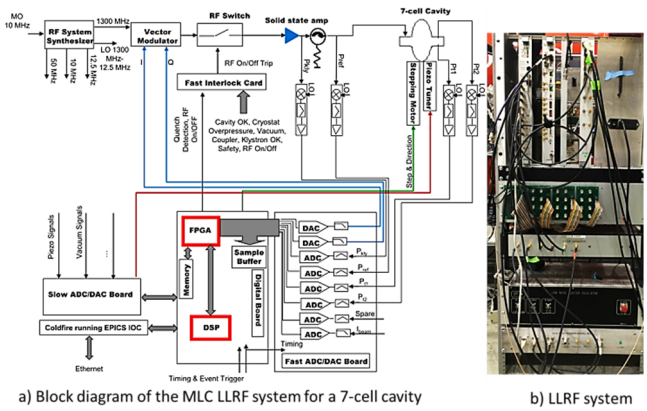

a) Block diagram of the MLC LLRF system for a 7-cell cavity b) LLRF system

Figure 2: a) Block diagram of the MLC LLRF system for a 7-cell cavity. b) Photograph of LLRF system hardware.

Measurement Results and Analysis

During the measurements, the frequency detuning versus time was recorded, and then the data was transformed into frequency domain by a Fourier transform as is shown in Fig. 3. The results show microphonics spectra with strong excitations near 30Hz, 60Hz, 90Hz, etc.

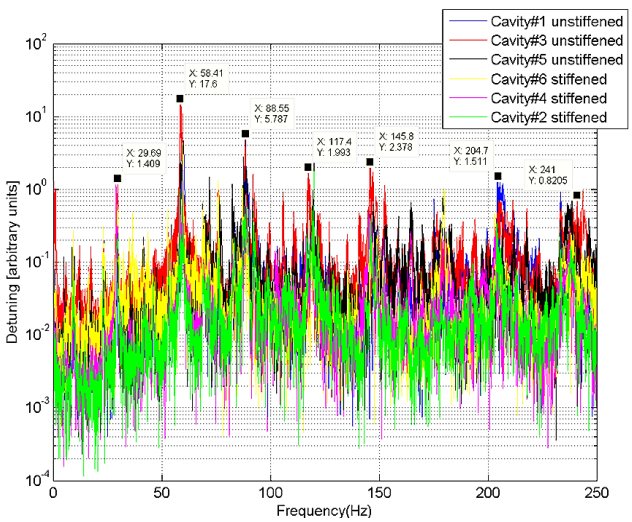

Figure 3: Cavity microphonics spectrum showing strong mechanical excitation at certain distinct frequencies.

To compare the microphonics levels in the individual cavities, the cavity detuning have been sampled and plotted in a histogram; see Fig. 4. As can been seen from these results, the average peak detuning of the three unstiffened cavities is ~100Hz, which is 2.5 times larger than for the three stiffened cavities (~40Hz).

An integrated detuning spectrum [9] gives a good visualization of the influence of each mechanical vibration excitation, defined by Eq. (3),

$$\Delta f_{rms}(f_{mod,n}) = \frac{\sqrt{\sum_{i=1}^{n} |\mathcal{F}[\Delta f(t)]_i|^2}}{\sqrt{2}}), \qquad (3)$$

where $\Delta f_{rms}(f_{mod,n})$ is the integrated detuning spectrum up to the modulating frequency of index n of the Fourier components $\mathcal{F}[\Delta f(t)]_i$. The results in Fig. 5 show that the integrated detuning strongly increases at ~60Hz, the frequency of the 120VAC. This, together with the ~30 Hz harmonics shown in the detuning spectrum, implies that these vibrations are driven by mechanical pumps, e.g. vacuum pump powered by 120VAC.

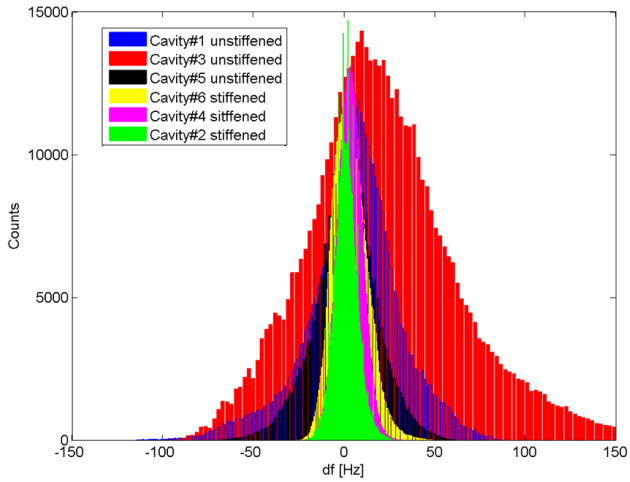

Figure 4: Histogram of the sampled detuning events of each cavity.

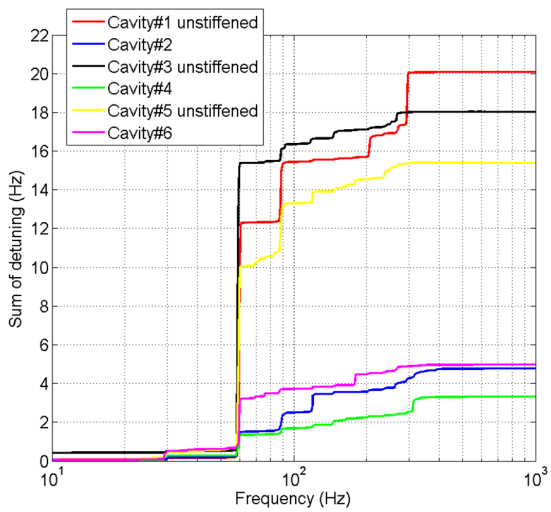

Figure 5: Integrated detuning amplitude showing that the 60Hz excitation is strongly contributing to the MLC microphonics.

It has to be pointed out that the measurements were carried out in a "mechanically noisy" environment. Tight scheduling for the initial test did not allow for isolating the cryomodule from ground vibrations present in the local environment. Additionally, liquid helium pumping

ISBN 978-3-95450-169-4

speed control and 80K high pressure helium gas cooling flow inside the MLC were not adequately optimized. Therefore, the measurement data reflects the worst-case microphonics level without any optimization and compensation.

The maximum energy gain of the MLC with the current microphonics levels has been calculated by Eq. (1) as shown in Fig. 6. The loaded-Q of the cavities could be further reduced to $Q_L \sim 2 \times 10^7$ using a 3 stub waveguide tuner to increase the maximum possible energy gain. Here $R/Q = 774\Omega$; $Q_0 = 2 \times 10^{10}$. It requires ~3kW RF power to provide the nominal 36MeV energy gain with $Q_L \sim 6 \times 10^7$; while ~2kW would be sufficient with reduced Q_L.

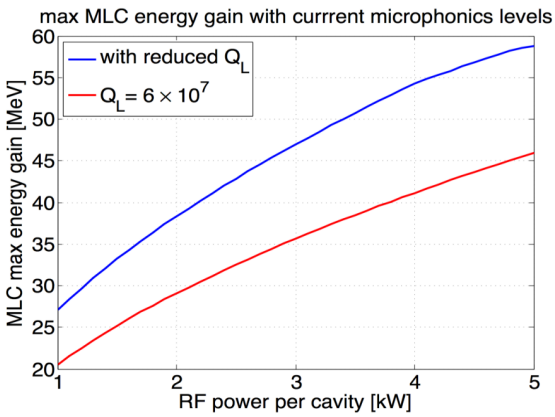

Figure 6: Maximum total energy gain of the MLC versus RF power available per cavity, assuming current microphonics levels.

MICROPHONICS SOURCES ANALYSIS

Investigation of the microphonics sources has started. We turned on and off equipment around the MLC one by one, and compared the changes of microphonics levels to identify the sources. Some dominant sources we noticed are the 2K pumping skid and the insulation vacuum pump, as is shown in Fig. 7. With the pump skid off, microphonics was measured at two values for the 80K high pressure helium flow, 7.5 g/s and 2.4 g/s. Vibrations at 30Hz and 90Hz were reduced at the lower flow rate as is shown in Fig. 7 b). The strong microphonics line at 60Hz disappeared when we shut down the insulation vacuum pump, as is shown in Fig.7 c).

As shown in Fig. 8, there are two ways that the vibrations can couple to the cavities: 1) the mechanical vibrations, including broadband machinery noise as well as narrow bandwidth sources like vacuum, water pumps, can couple through the beam-pipes and the cavity support structure; and 2) pressure fluctuations and waves in the liquid helium 2K2P line (e.g. due to JT value actuation) can transmit to the cavities through the LHe.

The analysis above informs our next steps to strongly reduce detuning from microphonics. 1) Optimize the 2K pumping control loop. 2) Fix the position of the JT and regulate the liquid level with the 2K2P heater. 3) Optimize the high pressure helium flow rates in the 80K tubing. 4) Isolate the beam line with weights and bellows from the outside. 5) Reduce mechanical coupling of the insulation vacuum pump top the MLC. 6) Explore fast piezo tuner based microphonics compensation.

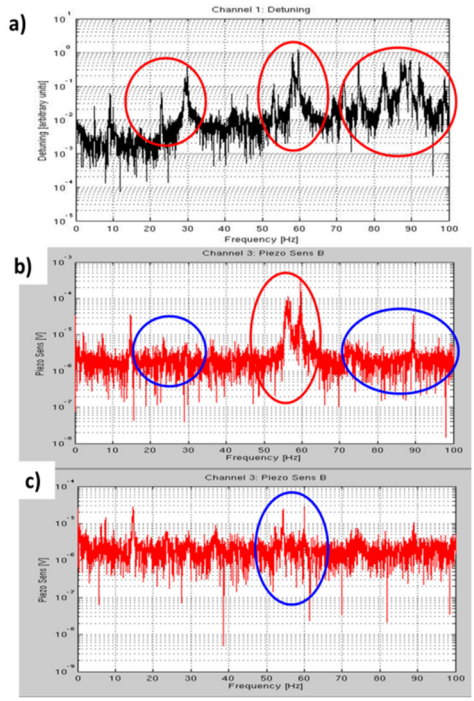

Figure 7: Results of microphonics sources analysis, a) showing the microphonics without optimization and compensation; b) the microphonics at 30Hz and 90Hz have been reduced when the 2K pump skids were turned off and the flow rate in 80K line was reduced; c) when the insulation vacuum pump was shut down the microphonics at 60Hz was decreased.

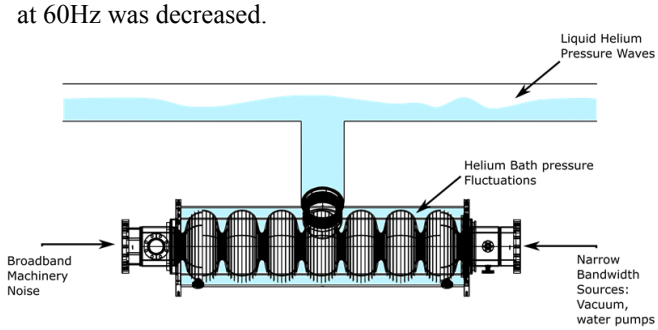

Figure 8: Diagram of a 7-cell cavity with cryogenic structure showing mechanical vibration propagating through the cavity beam-pipes as well as liquid-helium pressure fluctuation imposed on the cavity body.

CONCLUSION

Microphonics measurements were carried out in a "mechanically noisy" environment and without applying fast tuner compensation. With the current detuning level the MLC can provide 36MeV energy gain (CBETA specification) at 2-3kW RF power per cavity without beam loading.

REFERENCES

[1] I. Bazarov, *et al.*, "The Cornell-BNL FFAG-ERL Test Accelerator: White Paper", arXiv:1504.00588 (2014).

[2] G. Hoffstaetter, D. Trbojevic (eds.), "CBETA Conceptual Design Report", unpublished.

[3] E.C. Aschenauer, *et al.*, "eRHIC Design Study: An Electron-Ion Collider at BNL", arXiv:1409.1633 (2014).

[4] R. Eichhorn, *et al.*, "High Q Cavities for the Cornell ERL Main Linac", in *Proceedings of SRF2013*, Paris, France, Sept. 2013, paper THIOB02, pp. 844-849.

[5] F. Furuta, *et al*., "ERL Main Linac Cryomodule Cavity Performance and Effect of Thermal Cycling", in *Proceedings IPAC2016*, Busan, Korea, May. 2016, paper WEPMR022, pp.2313-2315.

[6] F. Furuta, *et al*., "Performance of the Novel Cornell ERL Main Linac Prototype Cryomodule", presented at *LINAC 2016*, East Lansing, MI USA, Sept. 2016, paper TUPLR011, this conference.

[7] G. Hoffstaetter, S. Gruner, M. Tigner (eds.), "The Cornell Energy Recovery Linac: Project Definition Design Report", (2013).http://www.classe.cornell.edu/Research/ERL/PDDR.html

[8] S. Posen, M. Liepe, "Mechanical optimization of superconducting cavities in continuous wave operation", *Phys. Rev. ST Accel. Beams*, vol. 15, p. 022002, 2010.

[9] A. Neumann, *et al*., "Analysis and active compensation of Microphonics in continuous wave narrow-bandwidth superconducting cavities", *Phys. Rev. ST Accel. Beams*, vol. 13, p. 082001, Dec. 2010.

ISBN 978-3-95450-169-4